Modification of Neural Activity in the Rostral Region of the Posterior Hypothalamus in Response to Stress Habituation

By Lindsay Atkinson

Honor's thesis submitted to the

Psychology and Neuroscience Department

University of Colorado Boulder

April 8, 2024

Under the supervision of Serge Campeau, PhD

Committee Members:

Serge Campeau; Psychology and Neuroscience, Thesis Advisor

Susanna Molas; Psychology and Neuroscience, Honor's Council Representative

Harrison Carpenter; Ecology and Evolutionary Biology, Outside Reader

Table of Contents

Abstract

Excessive or chronic stress is correlated with many common physical and mental disorders. With stress being a widespread experience in today's society, the ability to adapt to stress is important to limit its cumulative harmful impact. One form of adaptation is stress habituation, where a reduction in both sympathetic nervous system and hypothalamic-pituitary-adrenal axis activation is seen in response to repeated presentations of the same (homotypic) stressful situation over time. The neural mechanism of habituation is poorly understood, but evidence points towards involvement of the rostral region of the posterior hypothalamus (rPH) contributing to the habituation process. This study is interested in confirming that role by measuring calcium influx, as an index for neuronal activity, in the rPH of Sprague Dawley rats before and after audiogenic stress habituation. Calcium influx was measured using GCaMP by detecting fluorescence emission from Green Fluorescent Protein as calcium ions enter the cell and the intensity of fluorescence was evaluated using fiber photometry. The rPH was observed to have a reduction in calcium signaling from before to after habituation to a loud noise stressor, but that reduction was not observed for stimuli that were not repeatedly presented. With the calcium signal reduction interpreted as a reduction in the region's activity, this study provides additional evidence that the rPH contributes to the mechanism of stress habituation.

Introduction

Stress is an adaptive mechanism producing significant responses in both physiology and psychology in response to a real or perceived threat. Typically, these responses are beneficial by providing the motivation and the physiologic and physical means to meet the challenges of daily stressors that threaten to disrupt homeostasis, but these stress systems and their responses can become harmful when the stress is repeated or chronic. Excessive or chronic stress has been linked to mental disorders such as PTSD, anxiety, and depression, as well as physical disorders such as obesity, cardiovascular disease, Alzheimer's disease, and more (Kessler, 1997; McEwen, 2000). In particular, negative health effects can emerge following some cases of repeated stress by resulting in the sensitization of stress response systems (Post, 2016 ; McEwen, 2000). In cases where moderate repeated stress is the same (homotypic), however, a reduction in stress response activation over time is observed (Hughes et al., 2018). This adaptation is mediated by a form of nonassociative learning characterized by the reduction in magnitude of response to a moderate-intensity stimulus when the stimulus is presented repeatedly, termed habituation (Grissom & Bhatnagar, 2009; Thompson & Spencer, 1966). Habituation to homotypic stress is likely important to reduce the cumulative impact of similar daily stressors, combating mental and physical disease commonly correlated with excessive stress. Impairments to an organism's stress habituation, then, result in longer, more frequent, and more extreme activation of stress response systems (Metzger et al., 1999). Additionally, impairments in stress habituation specifically show correlations with the development of mood/anxiety disorders, adrenal hypertrophy, stomach ulcers, and more (Chattopadhyay et al., 1980; Reus et al., 1985; Paré, 1964; Golier et al., 2007; Simeon et al., 2007; Turner et al., 2020). The neural mechanisms that mediate the process of habituation are currently poorly understood. Investigation identifying habituation neurocircuitry

is important for further developing understanding of stress on physical and mental health, and for developing more effective treatments for stress-related disorders.

There are two major systems that respond to real or perceived homeostatic threats: the sympathetic nervous system (SNS) and the hypothalamic-pituitary-adrenal (HPA) axis. The SNS offers a rapid "fight-or-flight" response to stress, such as an increase in heart rate and blood pressure, facilitated by neural innervation of norepinephrine on receptors of target organs. The HPA axis, in contrast, offers a relatively slow but more sustained hormonal change in physiology to meet the potential increased energetic demands under many stress conditions. The HPA axis produces effects by neuroendocrine activation of the paraventricular nucleus of the hypothalamus (PVN) ultimately resulting in increased levels of glucocorticoids from the adrenal cortex into the bloodstream (cortisol for humans and corticosterone for rodents). Both SNS and HPA axis responses have been shown to habituate to repeated homotypic stress, suggesting that there may be a specific neural region responsible for the habituation of both systems (Armario et al., 1984; De Boer et al., 1988). Although previous research has targeted the PVN due to indication of involvement in initiating both SNS and HPA response systems, evidence now points towards the rostral region of the posterior hypothalamic nucleus (rPH) due to its relatively stronger sensitivity in activation of both systems (DiMicco et al., 2002). The rPH is found to receive extensive projections originating from the prefrontal cortex, amygdala, and other areas of the limbic system involved in regulation of stress responsivity. It then also projects to various nuclei of the hypothalamus, brainstem, and medulla, including the PVN and regions involved in sympathetic and behavioral responses, suggesting its role in stress response system activation. Together, the rPH integrates information from regions responsible for risk/threat assessment and behavioral and physiological stress reactions, suggesting that it may be important for stress

adaptation (DiMicco et al., 2002; Kataoka et al., 2014; Myers et al., 2016; Nyhuis et al., 2016). Additionally, this region has been found to be necessary for habituated stress responses and has shown development of differential mRNA regulation in response to repeated homotypic stress (Nyhuis et al., 2016; Campeau et al., 2023).

In the current study, we were interested in confirming a role of the rPH during habituation to repeated homotypic stress by measuring intracellular calcium ion signaling, as an index of neuronal activity, in rPH neurons during habituated stressful events in rats. To do this, we injected Genetically Encoded Calcium Indicators (GCaMP) into the rPH which indicates calcium concentration changes by expressing Green Fluorescent Protein (GFP) fluorescence in response to calcium binding to the binding protein calmodulin. This fluorescence was measured by fiber photometry using Tucker Davis Technologies instrumentation. We used loud noise as the moderate stressor in this study due to previous evidence of audiogenic stress prompting stress-related responses, and those responses habituating with multiple exposures (Nyhuis et al., 2016). The subjects' intracellular rPH calcium signal in response to loud noise was measured during an initial test day in order to collect baseline rPH activity levels when presented with audiogenic stress. The subjects then underwent six days of repeated stress exposures, experiencing thirty minutes of sustained loud noise each day. On the final test day, the subjects again underwent fiber photometry to determine the effect of habituation to the stressor on rPH activity levels. rPH activity in rats, as interpreted from calcium signaling, was hypothesized to be reduced from the first to last loud noise exposure test after having six days of repeated loud noise presentations. Some control conditions tested the possibility that rPH activity might simply change over time regardless of experiencing habituation, by presenting moderately stressful conditions (tail

pinches and bright light exposure) but without repeatedly exposing the subjects to these conditions between the initial and last test day.

Methods

Animals

Nine male and nine female adult (approximately 3-6 months old) Sprague Dawley rats (weighing 225-646g for males; 200-408g for females) were used. These animals were naïve to the experimental conditions of the current study. After animals were obtained from a vendor (Inotiv, formerly Envigo) or after use as breeders by other CU Boulder investigators, they were acclimated to the colony for one week during which they were handled for several minutes daily to habituate them to human handling (see Figure 1 for the experimental timeline of the entire study). Rats were initially housed two per cage and singly after surgeries, in clear Plexiglas tubs containing saw dust, with wire rim tops that gave access to rat chow and water *ad libitum*. All procedures were approved by the Institutional Animal Care and Use Committee (IACUC) at the University of Colorado, Boulder (protocol #2573-1).

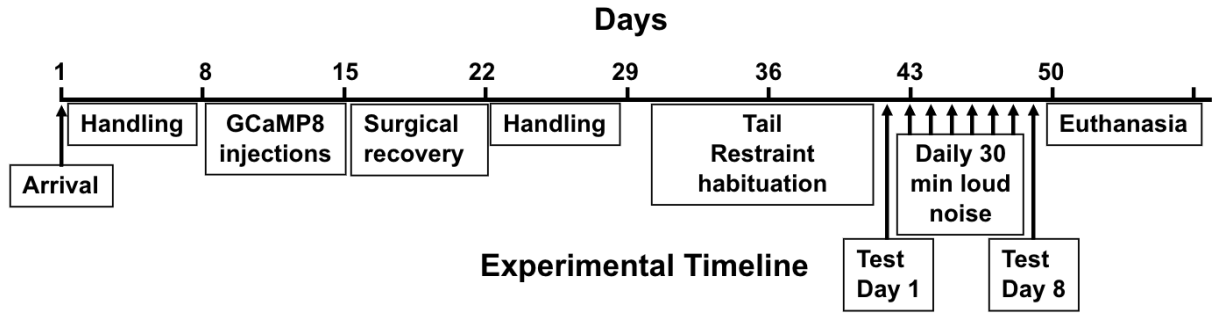

Figure 1: Timeline of experimental procedures.

Surgical Procedures

The surgical procedure was performed on anesthetized (isoflurane) rats and was conducted aseptically using the surgical tip method. A horizontal midline incision was made from between the eyes to the back of the skull. After retraction of the skin, a small window was then drilled into the skull to allow access of the injection needle containing 3.4 x 10^{12} vg/mL AAV1.Syn. jGCaMP8m.WPRE (#162375, Addgene) construct. The GCaMP virus was injected unilaterally at a rate of 100 ηl/min in a total volume of 500 µL, 3.3 mm posterior, 0.3 mm lateral, and 8.0 mm ventral to Bregma using the flat skull coordinates from the Paxinos and Watson stereotactic atlas (Paxinos & Watson, 2006). Optic fibers (400 µm core diameter, 0.66 NA, Doric Lenses) were then implanted at the same coordinates. The optic fibers were anchored in place using four cranial screws arranged on the skull around the surgical site and dental cement covering the screws and fiber implant. Following injections and fiber placement, the skin wound was closed with surgical staples as needed, the rats were injected with long-acting (72 hours) opiates (buprenorphine) and a non-steroidal anti-inflammatory analgesic for pain management (Meloxicam), anesthesia was discontinued, and the rats were kept under observation until ambulatory. A period of one week elapsed to allow animals to recover from surgery before beginning behavioral manipulations. Three male rats experienced complications with surgery recovery and had to be euthanized.

Behavioral Procedures

One week after surgery, rats were handled daily for a few minutes to reaccustom them to human handling (Figure 1). Following five days of handling, rats were habituated for five days to tail restraint procedures necessary for connecting the fiber optic sensor on photometry test days. Tail restraint consisted of gently wrapping approximately 2 inches of medical tape (1” diameter)

at the base of the tail while the rat was wrapped in a towel. The tail was then gently passed through a small opening at the base of an elevated Plexiglas platform, and taped to the back of the platform behind an additional Plexiglas wall such that rats could not access the taped portion of their tail. They were placed in the tail restraint device for 15 minutes on day 1, 20 minutes on day 2, and 25 minutes on days 3-5. After the tail restraint habituation, rats underwent one day of fiber photometry testing, then habituation to loud noise for six days, then a final fiber photometry test, as shown in Figure 1. For the loud noise habituation, rats, in their home cages, were presented with a loud noise (white noise, 10-50,000 Hz, 100 dB, A scale) for 30 minutes in custom-made soundproof boxes that were ventilated and lit. The fiber photometry test was performed under red light conditions (light intensity = 2.70-10 lux) where the rats were placed under tail restraint to allow for optic fiber connection for photometry. The two photometry tests consisted of a 37-minute session including two minutes of loud noise exposures (95dB, 100 dB, and 105dB, two exposures each) at an interstimulus interval of two minutes, followed by three tail pinches one minute apart, and finishing with three one-minute exposures to a bright white light (light intensity = 320-790 lux) with a one-minute interstimulus interval. Following the final day of fiber photometry, rats were euthanized with an overdose of sodium pentobarbital (Fatal Plus, Vortech Pharmaceuticals, MI), and rapidly perfused transcardially with ice-cold solutions consisting of 100 mLs of 0.9% saline and 500 mLs of 4% paraformaldehyde in 0.1 M sodium phosphate buffer, pH 7.4. Brains were removed, soaked into the same 4% paraformaldehyde solution for an additional 24 hours, transferred into a solution of 30% sucrose in 0.1 M sodium phosphate buffer (pH 7.4) for 7-10 days and frozen for later sectioning (40μm) and analysis of GCaMP expression and optic fiber placement.

Microscopic Data Acquisition and Image Analysis

The slides were observed for the presence of the fluorescent protein Green Florescent Protein (GFP) (emission spectrum ~509 nm) on a research microscope (Zeiss AxioImager). Epifluorescence images were captured of the brain tissue, and assessment of the viral infection spread together with the position of the optic fiber tip in the region of the rPH were completed. Digital records were obtained using the Zen Blue Edition 3.1 platform software from Zeiss.

Fiber Photometry Methodology

The calcium (GCaMP8m) sensor was recorded at two wavelengths, 465nm and 405nm isosbestic control, by amplitude modulated signals from two LEDs coupled into one optic fiber. Sensor signals and their isosbestic control emissions were returned through the same optic fiber and acquired using a femtowatt photoreceiver (Newport) and digitized (1 kHz; Tucker Davis Technologies). Behavioral timestamps were digitized by TTL input (Synapse software) of noise and light onset/offset and tail pinch. Raw data was analyzed with custom matlab scripts (available on Dr. Root's website). Signals (465nm and 405nm) were down sampled (10X) and peri-event time histograms were created for each stimulus exposure between -10 sec and +60 sec for the loud noise stimuli, between -10 sec and +30 sec for the light and tail pinch stimulations during the 1st and 2nd recording sessions (Day 1 and 8). For each recording session, data were processed such that the predicted 405nm channel was subtracted from the 465nm signal to remove movement, photo-bleaching, and fiber bending artifacts (dF). Normalized dF were calculated by z-scoring each stress exposure, where the mean and standard deviation of the z-score were calculated between -10 to 30 or 60 seconds.

Statistical Analysis

To analyze photometric results on the obtained z-scores, two methods were employed; the respective peak baseline normalized dF (between -5 to 0 seconds) values were compared to

loud noise, light, and tail pinch normalized dF (between 0 to +3 seconds) values, which were computed for each animal and each stimulus exposure. An average of all the loud noise, tail pinch, and light trials, respectively, were computed for each animal such that each subject in the study had single baseline and peak values for each trial type. The second method calculated areas under the curve (AUCs) for baseline normalized dF (between -5 to 0 seconds) compared to loud noise, light, and tail pinch normalized dF (between 0 to +3 seconds) for each animal and stimulus exposures, respectively. Again, an average of all the loud noise, light, and tail pinch trials, respectively, were computed for each animal such that each subject in the study had a single baseline and stimulated value for each trial type. Repeated measures analyses of variances (ANOVA) with sex (female vs. male), day (test day 1 vs. day 8), and condition (baseline vs. stimulated) were calculated for the peak and AUC values, respectively. Because no effects of sex were observed in initial analyses, similar repeated measures ANOVA without sex were performed to increase the power of the tests. Correlation analyses (Pearson's product-moment correlations) were computed to determine if distance from rPH and GFP-positive cell densities were related to either peak responses, area under the curve, or two indices of loud noise habituation, defined as peak z-score of loud noise on Day 1 minus Day 8, or area under the curve for loud noise z-scores from Day 1 minus Day 8. All statistical analyses were performed in the R Studio environment (2023.12.1 Build 402) of the R program (ver. 4.3.0), and significance was set at $p \leq 0.05$.

Results

Anatomical results

GCaMP expression at the viral injection area was observed post-euthanasia by counting GFP tagged cells in brain sections. Most animals displayed fluorescence, though the density of

expression varied between animals with a range of 51-703 cells/mm^2 under the fiber tip. There were three animals that showed minimal GFP-positive cells (38-89 cells/mm^2) as well as poor stimulus-induced calcium modulation through photometry, and these animals' results have been separated from the rest of the animals in the study. The location of GFP tagged cells varied slightly for each animal depending on injection accuracy. Figure 2 shows an example of fiber optic placement and viral expression including the range of cells surrounding the fiber tip (red area under the tip) amenable to detection by photometry (Pisano et al., 2019).

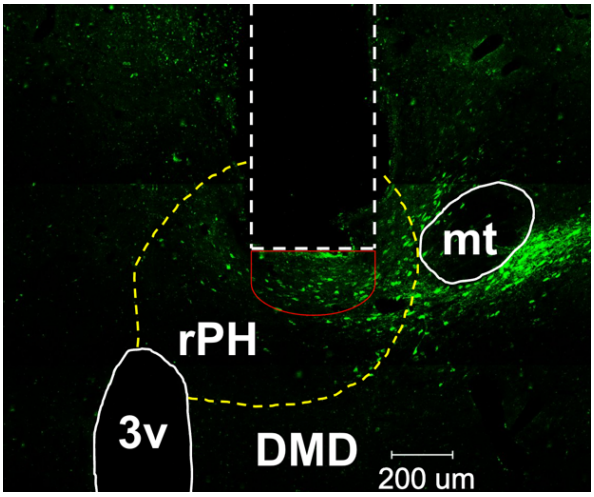

Figure 2: Representative optic fiber placement and green-fluorescent protein (GFP) signal indicating the likely presence of GCaMP expression. Dashed white line indicates fiber tract, area outlined in red represents estimated calcium signaling photometry range, and dashed yellow outline indicates rPH area. DMD: Dorsal region of the Dorsomedial nucleus of the hypothalamus; mt: mammillothalamic tract; rPH: rostral region of the posterior hypothalamic nucleus; 3V: third ventricle.

Optic fiber placement was analyzed to determine proximity to rPH target. Fiber placement varied slightly per animal, as shown in Figure 3. They were commonly placed slightly anterior to the rPH (between 0.1-1.1mm anterior) and ranged above and below the target area (between -0.45 to 1.8mm ventrodorsal to target rPH region at 3.3 mm caudal to Bregma). The

animals that did not show modified calcium signaling in response to stimulation are indicated with red dots (females) and squares (males).

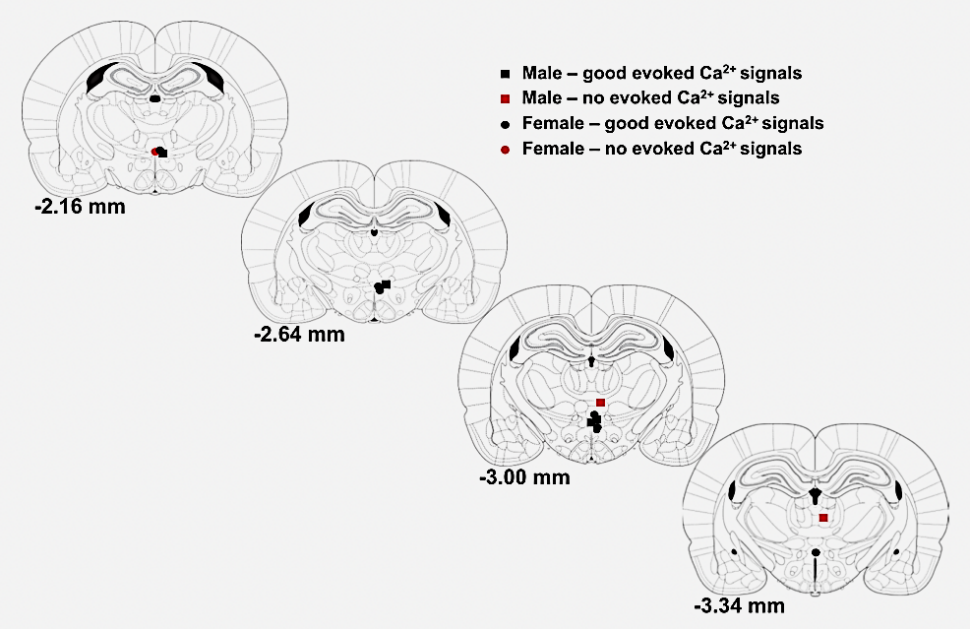

Figure 3: Representation of optic fiber tip placement for all animals shown on four rat brain sections between -2.16mm to -3.34mm posterior from Bregma. Female rats are indicated with a round dots, while males are represented by square dots, with dots in red indicating rats displaying little to no stimulus-induced calcium signaling.

Photometric results

This study included both male and female animals in order to assess the potential similarities or differences of photometry test results between sexes. Repeated-measure ANOVAs were performed comparing maximum photometry and AUC values between male and female animals for all three stimuli. There were no calculated interaction effects of sex on peak or AUC values across test day, test condition, or test day and condition interaction, for all trial types. The only area that showed some level of effect due to sex was the AUC values across test day for the tail pinch stimulus, but this effect still did not reach significance ($F_{(1,10)} = 4.812$, $p = 0.053$), suggesting no difference in photometry results between sexes. Since there were no observed

differences, both sexes have been grouped together for all subsequent tests in order to increase statistical power.

To determine general efficacy of stimulus-induced calcium signaling recording, graphs of photometric test results were generated. Fiber photometry test results for all animals showing stimulus-induced calcium changes (n=12) were averaged per stimulus type (noise, tail pinch, or light), producing graphs of z-scores comparing baseline calcium signaling (-10 to 0 seconds before stimulus onset) to calcium signaling after stimulus onset (0 to +60 seconds for loud noise, 0 to +30 seconds for light and tail pinch) as shown in Figure 4A-C. Average results for the first and last days of photometry testing were compared. For all three stimuli, calcium signaling was shown to sharply increase at stimulus onset, then quickly decrease, and finally level off near baseline. The increase at stimulus onset indicates effective stimulus-induced signal modulation. Figure 5A-C show the same graphs but instead using photometric data from animals without stimulus-induced signals (n=2 to 3), which show no increase in calcium signaling in response to stimuli.

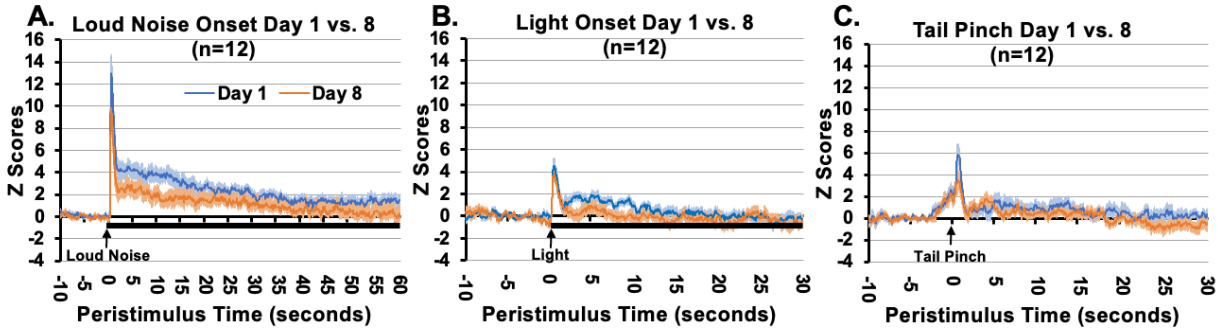

Figure 4: Average rPH calcium signal for animals with stimulus-induced calcium changes (n=12) measured by photometry for -10 seconds before to 60 seconds after stimulus onset for the first (Day 1 - blue) and the last (Day 8 - orange) test day. Calcium signal intensity is measured as z-scores in relation to signal intensity baseline (-10 to 0 seconds before stimulus onset). **A.** Average rPH calcium signal for the loud noise stimuli. **B.** Average rPH calcium signal for the light stimuli. **C.** Average rPH calcium signal for the tail pinch stimuli.

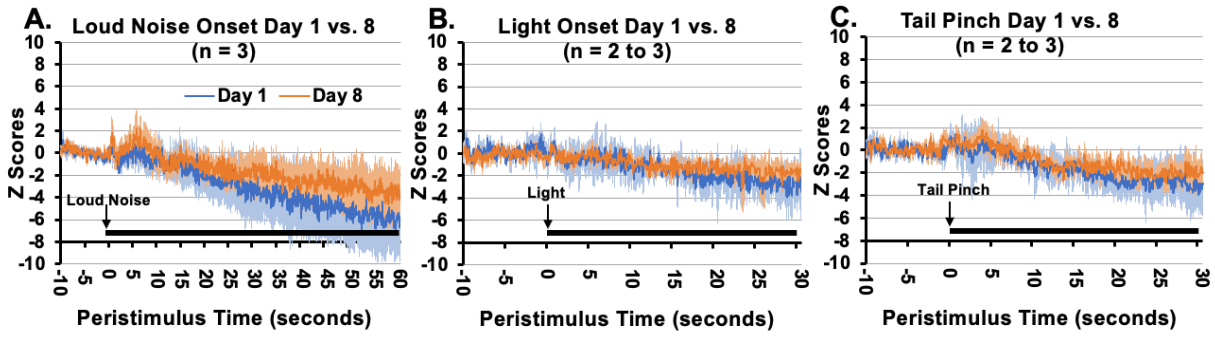

Figure 5: Average rPH calcium signal for animals without stimulus-induced calcium changes (n=2 to 3) measured by photometry for -10 seconds before to 60 seconds after stimulus onset for the first (Day 1 - blue) and the last (Day 8 - orange) test day. Calcium signal intensity is measured as z-scores in relation to signal intensity baseline (-10 to 0 seconds before stimulus onset). **A.** Average rPH calcium signal for the loud noise stimuli. **B.** Average rPH calcium signal for the light stimuli. **C.** Average rPH calcium signal for the tail pinch stimuli.

To evaluate the effect of habituation on photometry results, two maximum photometry values were extracted for each animal, one within -5 to 0 seconds before stimulus onset as their basal signal and one within 0 to +3 seconds after stimulus onset as their peak signal, for both the first and last days of photometry testing and for each trial type. Average maximum values are displayed in Figure 6A-C for animals with calcium changes in response to stimuli, and Figure 7A-C for animals with no stimulus-induced calcium changes. Note that one of the 3 rats in Figure 7 escaped following the first tail pinch of test Day 1, reducing the number of observations to 2 for the light and tail pinch stimuli.

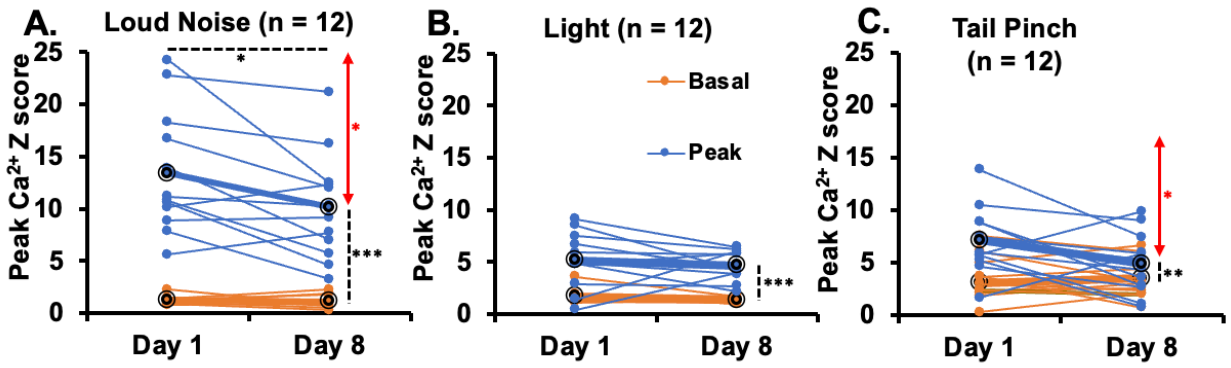

Figure 6: Maximum basal or peak calcium signal photometry values as z-scores from baseline for each animal that showed stimulus-induced calcium changes (n=12) including change in signal intensity between the first (Day 1) and last (Day 8) day of photometry testing. Average signal intensities for each condition and day are shown by black circles. Dashed black horizontal line represents significant effects across days, dashed black vertical line represents significant effects across conditions, and red vertical line represents significant test day and condition interaction. **A.** Maximum photometry results for the loud noise stimuli. **B.** Maximum photometry results for the light stimuli. **C.** Maximum photometry results for the tail pinch stimuli. *$p < 0.05$, **$p < 0.01$, ***$p < 0.001$.

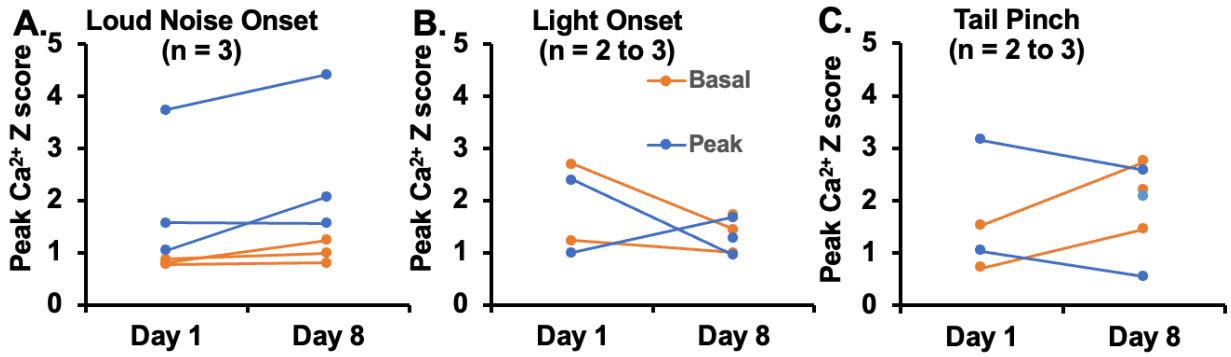

Figure 7: Maximum basal or peak calcium signal photometry values as z-scores from baseline for each animal not showing stimulus-induced calcium changes (n=2 to 3) including change in signal intensity between the first (Day 1) and last (Day 8) day of photometry testing. **A.** Maximum photometry results for the loud noise stimuli. **B.** Maximum photometry results for the light stimuli. **C.** Maximum photometry results for the tail pinch stimuli.

Repeated measures ANOVA were performed on maximum values for animals with stimulus-induced changes for each stimulus type to determine effects of testing day and

condition (basal and peak signal levels). Beginning with loud noise, an overall effect of test day was observed across basal and peak conditions ($F_{(1,11)} = 7.11$, $p = 0.022$), indicating that there were different photometry results between the first and last testing days. An effect of the basal and peak conditions was also found across both testing days ($F_{(1,11)} = 52.11$, $p = 1.71e\text{-}05$), demonstrating an overall influence of the loud noise stimulus on calcium signaling. Finally, there was a significant interaction of test days and conditions ($F_{(1,11)} = 7.865$, $p = 0.017$). Paired t-tests were performed to determine whether the basal or the peak photometry values demonstrated significant difference between test days, therefore contributing to the interaction. Results indicated that peak photometry values were significantly different between the first and last testing day ($t_{(11)} = 2.7641$, $p = 0.018$) but basal values were not ($t_{(11)} = 0.66143$, $p = 0.52$), implying lower rPH responses to the loud noise stimuli on Day 8 (see Figure 6A). Peak and basal signaling in response to light, in contrast, showed no significant effect of test day on basal and peak values ($F_{(1,11)} = 0.924$, $p = 0.36$) and no effect of test day and condition interaction ($F_{(1,11)} = 0.035$, $p = 0.86$), indicating that there was no change in basal/peak values between test days. There was a significant effect of condition across days ($F_{(1,11)} = 47.32$, $p = 2.66e\text{-}05$), however, demonstrating that the light stimuli did produce a significant calcium signaling change compared to basal conditions. Finally, the effect of test day on conditions for the tail pinch stimulus was found to be insignificant ($F_{(1,11)} = 1.279$, $p = 0.28$). There was an effect of condition across test day ($F_{(1,11)} = 15.03$, $p = 0.0026$), indicating that the tail pinch produced a difference in photometry signal. There was also an observed effect of test day and condition interaction ($F_{(1,11)} = 13.26$, $p = 0.0039$), with the peak measures differing significantly across test days ($t_{(11)} = 2.2034$, $p = 0.05$) but not the basal measures ($t_{(11)} = -0.58526$, $p = 0.57$).

Areas under the curve (AUC) were calculated for each stimulus type and test day as an additional method of determining effects of condition and day. For each trial type, the basal AUC value was calculated for -5 to 0 seconds before the stimulus onset and the stimulus AUC value was calculated for 0 to +3 seconds after stimulus onset, then submitted to a repeated-measures ANOVA for analysis. Average AUCs for each stimulus type is shown in Figure 8A-C for animals with stimulus-induced signal modulation, and Figure 9A-C for animals without stimulus-induced signal modulation.

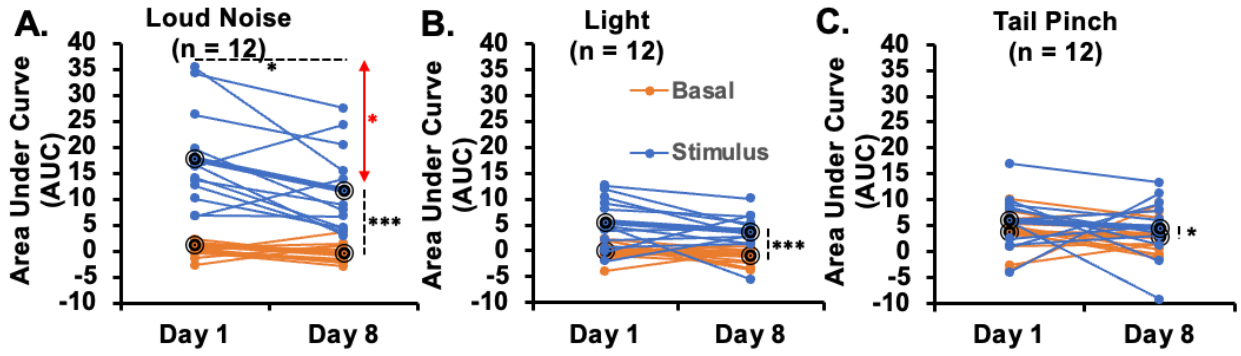

Figure 8: Basal or stimulus AUC values as z-scores from baseline for each animal with stimulus-induced changes (n=12) including change in signal intensity between the first (Day 1) and last (Day 8) day of photometry testing. Average AUC for each condition and day are shown by black circles. Dashed black horizontal line represents significant effects across days, dashed black vertical line represents significant effects across conditions, and red vertical line represents significant test day and condition interaction. **A.** AUC results for the loud noise stimuli. **B.** AUC results for the light stimuli. **C.** AUC results for the tail pinch stimuli. *$p < 0.05$, **$p < 0.01$, ***$p < 0.001$.

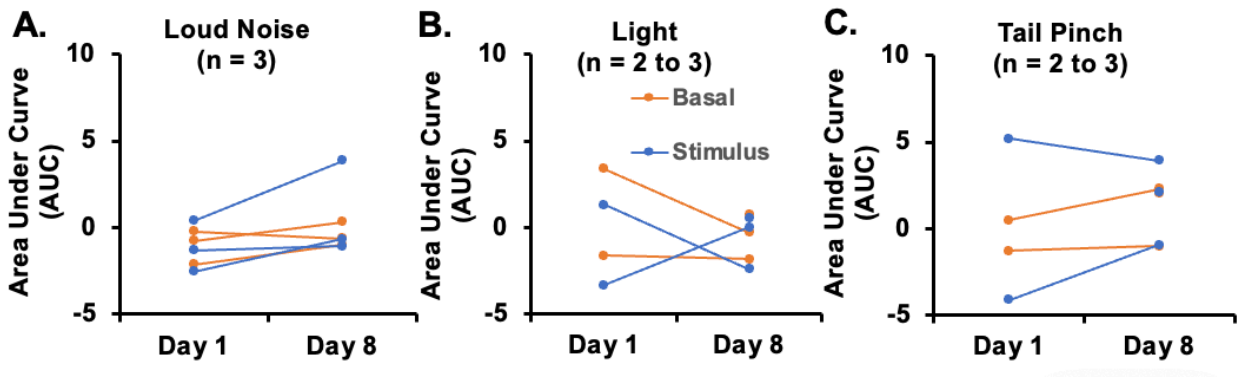

Figure 9: Basal or stimulus AUC values as z-scores from baseline for each animal without stimulus-induced changes (n=2 to 3) including change in signal intensity between the first (Day 1) and last (Day 8) day of photometry testing. **A.** AUC results for the loud noise stimuli. **B.** AUC results for the light stimuli. **C.** AUC results for the tail pinch stimuli.

In animals with stimulus-induced calcium modulation for loud noise, an overall effect of test day on AUC values was observed across conditions (basal and stimulus) ($F_{(1,11)} = 5.949$, $p = 0.033$), an overall effect of condition was observed across test day ($F_{(1,11)} = 42.57$, $p = 4.28e\text{-}05$), and there was a significant interaction between test day and condition ($F_{(1,11)} = 6.073$, $p = 0.031$). To determine which condition contributed to the interaction, paired t-tests were performed; the loud noise AUC was found to significantly vary between testing days ($t_{(11)} = 2.3593$, $p = 0.038$) but the basal AUC did not ($t_{(11)} = 0.55252$, $p = 0.59$), corresponding with the results calculated for loud noise maximum photometry values and again indicating lower rPH during test Day 8. Just like maximum values for the light stimulus, there was no observed effect of test day across conditions ($F_{(1,11)} = 1.807$, $p = 0.21$) and no effect of test day and condition interaction ($F_{(1,11)} = 0.632$, $p = 0.44$), but there was a significant effect of AUC condition across test days ($F_{(1,11)} = 24.59$, $p = 0.00043$). Finally, tail pinch showed no effect of test day across conditions ($F_{(1,11)} = 0.331$, $p = 0.58$) but a significant effect of condition across test days ($F_{(1,11)} = 5.824$, $p = 0.034$), as was seen with maximum values. Contrasting maximum signaling results, the tail pinch stimulus showed no significant test day and condition interaction for AUC ($F_{(1,11)} = 0.251$, $p =$

0.63). Results for the light and tail pinch stimuli suggest little to no changes in rPH activity across testing days. Correlations were computed between maximum peak and stimulus-AUC values for loud noise for each animal in order to confirm association between the two measurements of photometry results. This correlation was found to be significant (Pearson's r: 0.947, $t_{(13)} = 10.594$, $p = 9.18e\text{-}08$), meaning that, for each animal, a relatively high peak value is associated with a high AUC value, and a relatively low peak value is associated with a low AUC value.

Lastly, Pearson correlations between fiber tip placement (as distance from rPH) and magnitude of habituation in photometry results were computed to determine if fiber placement from the rPH had an effect on results. Across multiple measures of distance (rostral-caudal, ventral-dorsal, and total) and a habituation index of both peak and AUC photometry values in response to the loud noise stimulus, there were no significant correlations. The only relationship that did show a trend towards significance was the correlation between the vertical (ventral-dorsal) distance from the rPH and calculated habituation-AUC (Pearson's r: -0.504, $t_{(13)} = -2.1027$, $p = 0.055$), shown in Figure 10, suggesting that vertical proximity to the rPH may be associated with higher habituation index AUC in response to the loud noise stressor. Correlations between density of GFP infected cells and basal photometry results were also calculated to determine if the number of GFP-positive cells had an effect on baseline photometry, and the association did not quite reach significance (Pearson's r: 0.46601, $t_{(13)} = 1.899$, $p = 0.08$). Looking at raw photometry emission levels, there was a correlation between the intensity of emissions from the 465nm wavelength (exciting GFP) and density of GFP-tagged cells (Pearson's r: 0.51781, $t_{(13)} = 2.1824$, $p = 0.048$), but not for the 405nm isosbestic control

(Pearson's r: 0.44188, $t_{(13)} = 1.776$, $p = 0.099$). Raw photometry emissions, photometry results, fiber distance from the rPH, and GFP-tagged cell density for each animal are reported in Table 1.

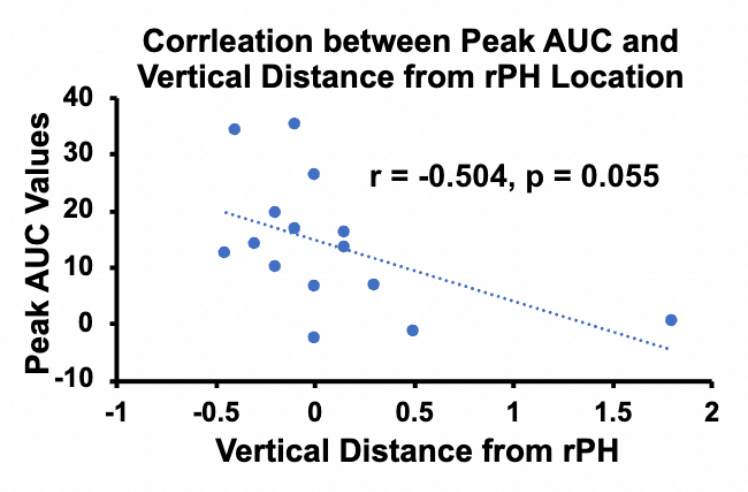

Figure 10: Correlation between optic fiber tip placement in vertical distance from the rPH and peak AUC values in response to the loud noise stimulus on the first day of photometry testing.

ID	Raw 465nm Fluor	Raw 405nm Fluor	Basal	Peak	AUC basal	AUC peak	Peak hab index	AUC Hab Index	Horiz distance	Vert distance	Cells/mm²
FFG8	**260**	**163**	**1.46**	**10.13**	**-0.51**	**16.16**	**-2.18**	**-8.07**	**0.9**	**0.15**	**511**
FFC1	**223**	**60**	**1.21**	**18.29**	**2.17**	**26.23**	**2.10**	**5.77**	**0.1**	**0**	**294**
FFC5	**257**	**169**	**1.11**	**8.85**	**0.42**	**6.78**	**-0.29**	**0.03**	**0.3**	**0.3**	**281**
FFC8	**317**	**167**	**0.92**	**24.23**	**-0.07**	**35.33**	**11.81**	**19.98**	**0.5**	**-0.1**	**268**
FFC9	**1145**	**527**	**1.30**	**16.69**	**0.67**	**13.57**	**4.67**	**4.71**	**0.9**	**0.15**	**703**
FFC10	**310**	**157**	**1.05**	**5.57**	**-2.74**	**6.64**	**-2.17**	**-7.14**	**0.1**	**0**	**435**
FFC11	**795**	**454**	**0.87**	**10.75**	**-1.45**	**19.62**	**5.06**	**11.79**	**0.8**	**-0.2**	**307**
FFC12	**551**	**485**	**1.32**	**11.18**	**0.69**	**10.04**	**0.88**	**5.82**	**0.1**	**-0.2**	**460**
FFC13	**638**	**324**	**1.42**	**22.81**	**-0.14**	**34.13**	**1.61**	**6.68**	**0.3**	**-0.4**	**256**
FFC14	**680**	**360**	**2.25**	**13.88**	**0.10**	**16.67**	**6.89**	**13.79**	**1**	**-0.1**	**435**
FFC17	**253**	**189**	**0.77**	**7.83**	**-0.18**	**12.54**	**4.61**	**8.82**	**1.1**	**-0.45**	**268**
FFC18	**245**	**210**	**1.36**	**10.56**	**1.25**	**14.01**	**5.99**	**9.59**	**0.7**	**-0.3**	**51**
FFC2	105	74	0.81	3.73	-0.76	0.39	-0.68	-3.46	0.1	1.8	38
FFC4	147	131	0.87	1.58	-0.23	-1.34	0.01	-0.24	0.3	0.5	64
FFC16	805	439	0.78	1.04	-2.12	-2.55	-1.03	-1.89	1.1	0	89

Table 1: Raw photometry emissions, photometry results, fiber distance from the rPH, and GFP-tagged cell density for each animal. Animals that showed stimulus-mediated calcium signaling have results shown in bold, and animals with poor stimulus-mediated calcium signaling have results in un-bolded text.

Discussion

The main goal of this experiment was to test stress adaptation mediated by habituation, a form of nonassociative learning where the magnitude of response to a moderate-intensity

stimulus is reduced when the stimulus is presented repeatedly (Grissom & Bhatnagar, 2009; Thompson & Spencer, 1966). Specifically, if stress habituation was to occur and be mediated by the rPH, a difference in calcium signaling (and therefore rPH activity levels) between the first and last days of photometry testing would be expected. This difference would only be expected for the loud noise stimulus because animals underwent habituation procedures for loud noise during the intervening photometric testing days, but habituation would not be expected to occur for tail pinch and bright light due to animals not being repeatedly exposed to those stimuli. Both peak and stimulus AUC values for loud noise onset were observed to be significantly lower on the last day of photometry testing compared to the first day, with the difference in calcium signaling suggesting involvement of the rPH in stress habituation. These results were specifically limited to stressor response, evidenced that maximum basal and basal AUC values were not found to change between the first and last testing day. In response to the light stimulus, habituation was not observed as expected; neither maximum peak and stimulus AUC nor maximum basal and basal AUC changed between the first and last testing day. The tail pinch stimulus produced ambiguous results; the peak photometry values in response to the tail pinch stimulus were significantly lower on the last test day compared to the first, however stimulus AUC values did not show a difference between testing days. Errors in stressor administration by the experimenter could have produced the differences in peak signaling observed. For example, tail pinches were administered manually which could have resulted in varied pinch intensities, and the experimenter could have administered the tail pinch a few seconds earlier or later than recorded which would produce errors with calcium signal and stimulus-onset alignment. Additionally, the animals were positioned in a way where they would be able to view the experimenter approaching to administer the tail pinch, which may have resulted in anticipatory

responses. The contradicting insignificant change in AUC values for the tail pinch stimulus also support the likelihood of significant peak signaling differences being due the limitations inherent with delivering tail pinch manually.

These photometry results were consistent across sex, supporting previous results from the Campeau lab of no effects of sex and implying that the habituation process is the same across males and females. Although this has been observed for stress habituation specifically, sex has been found to produce differences in overall stress responses and incidence of mood/anxiety disorders (Altemus et al., 2014; Johnston & File, 1991). The effects of sex, if any, should continue to be explored in stress and stress habituation research to determine which processes differ between males and females and which don't.

Although habituation to loud noise was seen via photometry results, it is important to verify that the habituation was mediated by the rPH specifically. Fiber implantation accuracy varied between animals, with most of the rPH "misses" being found in animals containing fibers that were anterior enough to reach the PVN. The PVN, being a region controlling the HPA axis, is expected to show a reduction in activity as HPA habituation occurs. Even though it does habituate, the PVN is not believed to be a component of the mechanism responsible for habituation (Herman, 2013; DiMicco et al., 2002). This may explain why no significant correlations between rPH accuracy and habituation results were found; most fiber placements for animals with stimulus-induced responses resulted in measurements close to the rPH or the PVN, both of which show habituation. There was one animal with a fiber placement dorsal to the target region and hitting neither the rPH nor the PVN, but that animal also showed poor stimulus-induced calcium signaling so it is unclear how that region's activity is affected by habituation. In future replications, a control group of animals with implants that are intentionally "missed"

outside of both the rPH and the PVN should be added in order to confirm that the rPH, and not other nearby regions that were not examined in this study, show evidence of habituation.

Also affecting photometry results, animals showed variable cell densities with fluorescent emissions and presumably, GCaMP infection. Green fluorescence protein infection densities were observed in brain sections under the microscope, and viral infection location was interpreted based on the GFP fluorescence visible. However, the GFP-positive cells that were visible in brain sections likely represent cells that were active at the time of euthanasia and may not include all virally infected cells expressing GCaMP. Animals may have also had difference in the overall activity of the region at the time of death, resulting in different densities of visibly infected cells. These possibilities may have produced a skewed representation of GCaMP injection location and/or infection density. Animals that showed minimal stimulus-induced calcium changes showed much less GFP-positivity in brain sections than most animals with stimulus-induced changes, suggesting that there might have been errors with GCaMP injection in those animals such as the injector being clogged, GCaMP injections and fiber implantations occurring in different locations, or injections using GCaMP virus with reduced efficacy in those animals. However, these animals still displayed sufficient “background” signaling, detecting some level of fluorescence present. The reason for these signaling results are unclear. Completing an immunohistochemistry stain for the GCaMP protein construct would provide a more accurate way to localize infected cells and confirm GCaMP infection densities, helping to explain the effects seen in animals showing minimal stimulus-mediated calcium signaling. This antibody was not available in the laboratory at the time of this project.

Although this study still does produce evidence supporting the rPH’s role in habituation, some additional limitations could be addressed. The procedures used in this study to induce

audiogenic habituation replicated previous procedures in the Campeau lab where successful habituation was confirmed (Nyhuis et al., 2016; Campeau et al., 2023), but this study did not directly measure habituation development. Since it is not clear that habituation had actually occurred, the difference between test days in calcium signaling in response to the loud noise stimulus could have been due to the stimulus type, mere chance, or some other mechanism altogether. Two procedure options could be employed in future replications to eliminate this unknown. First, blood samples and heart rate recordings could be taken along with photometry tests to determine changes in SNS activation and corticosterone levels between test days (Masini et al., 2011; Nyhuis et al., 2016), therefore confirming or denying the development of habituation. Secondly, a control group of animals could be added that would undergo both photometry tests as normal but not receive audiogenic habituation procedures in-between test days so that photometry results of animals that did and did not receive habituation could be compared.

Overall, findings from this study support other results gathered in the Campeau lab including the contribution of the rostral posterior hypothalamic nucleus in the development of stress habituation in rats (Nyhuis et al., 2016; Campeau et al., 2023), but the full neurocircuitry for habituation is still unknown. Learning more about the complete circuits and mechanism of habituation could help provide the basis for the development of treatments for stress-related disorders that target the habituation pathway. Now that increasing evidence suggests that rPH activity overall changes in response to habituation, some next questions that could be addressed include determining which distinct rPH cell populations mediate the reduction in rPH activity, and what are the specific mechanisms leading to this neural activity reduction. This study measured calcium signaling in a mixed cell population containing both neurons that use the

excitatory amino acid neurotransmitter glutamate, and others that employ the inhibitory amino acid neurotransmitter GABA, so there may be a differential change in signal modification in response to habituation depending on the cell population type. The signal reduction observed in this study could plausibly be mediated by a net increase in inhibitory activity or a net decrease in excitatory activity, both being possibilities to explore in future research. Overall, undergoing repeated stress can produce a wide variety of physical and mental health impairments and it is considered to be an influential predictor for various disease developments (Simeon et al., 2007; Munshi et al., 2020; Yuen et al., 2012; McEwen, 2000; Mousavi et al., 2023). It is important to provide attention to mechanisms in which the cumulative impact of repeated stress is reduced such as habituation, with stress being widespread and frequent among human experiences.

References

Altemus, M., Sarvaiya, N., & Neill Epperson, C. (2014). Sex differences in anxiety and depression clinical perspectives. *Frontiers in Neuroendocrinology*, *35*(3), 320–330. https://doi.org/10.1016/j.yfrne.2014.05.004

Armario, A., Castellanos, J. M., & Balasch, J. (1984). Adaptation of anterior pituitary hormones to chronic noise stress in male rats. *Behavioral and Neural Biology*, *41*(1), 71–76. https://doi.org/10.1016/s0163-1047(84)90745-3

Campeau, S., McNulty, C., Stanley, J. T., Gerber, A. N., Sasse, S. K., & Dowell, R. D. (2023). Determination of steady-state transcriptome modifications associated with repeated homotypic stress in the rat rostral posterior hypothalamic region. *Frontiers in Neuroscience*, *17*. https://www.frontiersin.org/articles/10.3389/fnins.2023.1173699

Chattopadhyay, P., Cooke, E., Toone, B., & Lader, M. (1980). Habituation of physiological responses in anxiety. *Biological Psychiatry*, *15*(5), 711–721.

De Boer, S. F., Slangen, J. L., & van der Gugten, J. (1988). Adaptation of plasma catecholamine and corticosterone responses to short-term repeated noise stress in rats. *Physiology & Behavior*, *44*(2), 273–280. https://doi.org/10.1016/0031-9384(88)90149-7

DiMicco, J. A., Samuels, B. C., Zaretskaia, M. V., & Zaretsky, D. V. (2002). The dorsomedial hypothalamus and the response to stress: Part renaissance, part revolution. *Pharmacology, Biochemistry, and Behavior*, *71*(3), 469–480. https://doi.org/10.1016/s0091-3057(01)00689-x

Golier, J. A., Schmeidler, J., Legge, J., & Yehuda, R. (2007). Twenty-four Hour Plasma Cortisol and Adrenocorticotropic Hormone in Gulf War Veterans: Relationships to Posttraumatic

Stress Disorder and Health Symptoms. *Biological Psychiatry*, *62*(10), 1175–1178. https://doi.org/10.1016/j.biopsych.2007.04.027

Grissom, N., & Bhatnagar, S. (2009). Habituation to repeated stress: Get used to it. *Neurobiology of Learning and Memory*, *92*(2), 215–224. https://doi.org/10.1016/j.nlm.2008.07.001

Herman, J. (2013). Neural control of chronic stress adaptation. *Frontiers in Behavioral Neuroscience*, *7*. https://doi.org/10.3389/fnbeh.2013.00061

Hughes, B. M., Lü, W., & Howard, S. (2018). Cardiovascular stress-response adaptation: Conceptual basis, empirical findings, and implications for disease processes. *International Journal of Psychophysiology*, *131*, 4–12. https://doi.org/10.1016/j.ijpsycho.2018.02.003

Johnston, A. L., & File, S. E. (1991). Sex differences in animal tests of anxiety. *Physiology & Behavior*, *49*(2), 245–250. https://doi.org/10.1016/0031-9384(91)90039-Q

Kataoka, N., Hioki, H., Kaneko, T., & Nakamura, K. (2014). Psychological Stress Activates a Dorsomedial Hypothalamus-Medullary Raphe Circuit Driving Brown Adipose Tissue Thermogenesis and Hyperthermia. *Cell Metabolism*, *20*(2), 346–358. https://doi.org/10.1016/j.cmet.2014.05.018

Kessler, R. C. (1997). The Effects of Stressful Life Events on Depression. *Annual Review of Psychology*, *48*(1), 191–214. https://doi.org/10.1146/annurev.psych.48.1.191

Masini, C. V., Nyhuis, T. J., Sasse, S. K., Day, H. E. W., & Campeau, S. (2011). Effects of voluntary wheel running on heart rate, body temperature, and locomotor activity in response to acute and repeated stressor exposures in rats. *Stress (Amsterdam, Netherlands)*, *14*(3), 324–334. https://doi.org/10.3109/10253890.2010.548013

McEwen, B. S. (2000). Allostasis and allostatic load: Implications for neuropsychopharmacology. *Neuropsychopharmacology: Official Publication of the American College of Neuropsychopharmacology*, *22*(2), 108–124. https://doi.org/10.1016/S0893-133X(99)00129-3

Metzger, L. J., Orr, S. P., Berry, N. J., Ahern, C. E., Lasko, N. B., & Pitman, R. K. (1999). Physiologic reactivity to startling tones in women with posttraumatic stress disorder. *Journal of Abnormal Psychology*, *108*(2), 347–352. https://doi.org/10.1037//0021-843x.108.2.347

Mousavi, M.-S., Meknatkhah, S., Imani, A., Geramifar, P., & Riazi, G. (2023). Comparable assessment of adolescent repeated physical or psychological stress effects on adult cardiac performance in female rats. *Scientific Reports*, *13*(1), 16401. https://doi.org/10.1038/s41598-023-43721-7

Munshi, S., Loh, M. K., Ferrara, N., DeJoseph, M. R., Ritger, A., Padival, M., Record, M. J., Urban, J. H., & Rosenkranz, J. A. (2020). Repeated stress induces a pro-inflammatory state, increases amygdala neuronal and microglial activation, and causes anxiety in adult male rats. *Brain, Behavior, and Immunity*, *84*, 180–199. https://doi.org/10.1016/j.bbi.2019.11.023

Myers, B., Carvalho-Netto, E., Wick-Carlson, D., Wu, C., Naser, S., Solomon, M. B., Ulrich-Lai, Y. M., & Herman, J. P. (2016). GABAergic Signaling within a Limbic-Hypothalamic Circuit Integrates Social and Anxiety-Like Behavior with Stress Reactivity. *Neuropsychopharmacology*, *41*(6), Article 6. https://doi.org/10.1038/npp.2015.311

Nyhuis, T. J., Masini, C. V., Day, H. E. W., & Campeau, S. (2016). Evidence for the Integration of Stress-Related Signals by the Rostral Posterior Hypothalamic Nucleus in the

Regulation of Acute and Repeated Stress-Evoked Hypothalamo-Pituitary-Adrenal Response in Rat. *The Journal of Neuroscience*, *36*(3), 795–805. https://doi.org/10.1523/JNEUROSCI.3413-15.2016

Paré, W. P. (1964). The Effect of Chronic Environmental Stress on Stomach Ulceration, Adrenal Function, and Consummatory Behavior in the Rat. *The Journal of Psychology*, *57*(1), 143–151. https://doi.org/10.1080/00223980.1964.9916683

Paxinos, G., & Watson, C. (2006). *The Rat Brain in Stereotaxic Coordinates: Hard Cover Edition*. Elsevier.

Pisano, F., Pisanello, M., Lee, S. J., Lee, J., Maglie, E., Balena, A., Sileo, L., Spagnolo, B., Bianco, M., Hyun, M., De Vittorio, M., Sabatini, B. L., & Pisanello, F. (2019). Depth-resolved fiber photometry with a single tapered optical fiber implant. *Nature Methods*, *16*(11), 1185–1192. https://doi.org/10.1038/s41592-019-0581-x

Post, R. M. (2016). Epigenetic basis of sensitization to stress, affective episodes, and stimulants: Implications for illness progression and prevention. *Bipolar Disorders*, *18*(4), 315–324. https://doi.org/10.1111/bdi.12401

Reus, V. I., Peeke, H. V. S., & Miner, C. (1985). Habituation and cortisol dysregulation in depression. *Biological Psychiatry*, *20*(9), 980–989. https://doi.org/10.1016/0006-3223(85)90196-9

Simeon, D., Knutelska, M., Yehuda, R., Putnam, F., Schmeidler, J., & Smith, L. M. (2007). Hypothalamic-Pituitary-Adrenal Axis Function in Dissociative Disorders, Post-Traumatic Stress Disorder, and Healthy Volunteers. *Biological Psychiatry*, *61*(8), 966–973. https://doi.org/10.1016/j.biopsych.2006.07.030

Thompson, R. F., & Spencer, W. A. (1966). Habituation: A model phenomenon for the study of neuronal substrates of behavior. *Psychological Review*, *73*(1), 16–43. https://doi.org/10.1037/h0022681

Turner, A. I., Smyth, N., Hall, S. J., Torres, S. J., Hussein, M., Jayasinghe, S. U., Ball, K., & Clow, A. J. (2020). Psychological stress reactivity and future health and disease outcomes: A systematic review of prospective evidence. *Psychoneuroendocrinology*, *114*, 104599. https://doi.org/10.1016/j.psyneuen.2020.104599

Yuen, E. Y., Wei, J., Liu, W., Zhong, P., Li, X., & Yan, Z. (2012). Repeated Stress Causes Cognitive Impairment by Suppressing Glutamate Receptor Expression and Function in Prefrontal Cortex. *Neuron*, *73*(5), 962–977. https://doi.org/10.1016/j.neuron.2011.12.033